

Synergy of oxygen defects and structural modulation on titanium niobium oxide with constructed conductive network for high-rate lithium-ion half/full batteries

Yangyang Sui^a, Jinpeng Guan^a, Kaiyang Li^a, Yubo Feng^a, Shengjie Peng^c, Maxim Yu.

Maximov^d, Quan Liu^{a*}, Jun Yang^{b*}, Hongbo Geng^{a*}

^aSchool of Materials Engineering, Changshu Institute of Technology, Changshu, Jiangsu 215500, China. E-mail address: njutlq@163.com; hbgeng@gdut.edu.cn

^bSchool of Material Science and Engineering, Jiangsu University of Science and Technology, Zhenjiang, 212003, China. E-mail address: iamjyang@just.edu.cn

^cCollege of Materials Science and Technology, Nanjing University of Aeronautics and Astronautics, Nanjing 210016, China

^dPeter the Great Saint-Petersburg Polytechnic University, 195251 Saint Petersburg, Russia

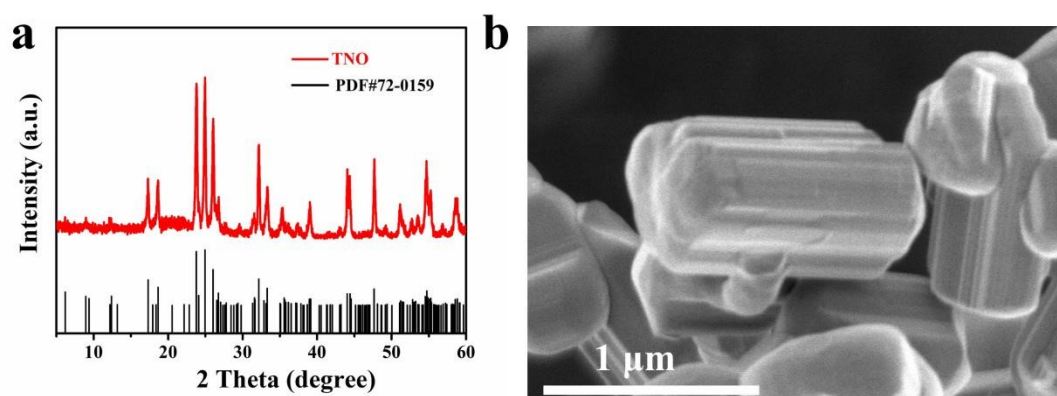


Fig. S1 Microstructure and morphology of TNO. (a) XRD pattern; (b) SEM images.

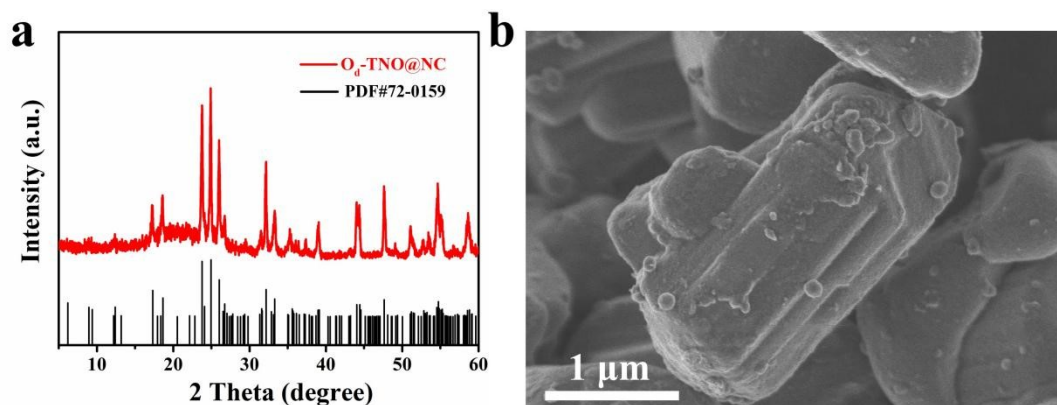


Fig. S2 Microstructure and morphology of O_d -TNO@NC. (a) XRD pattern; (b) SEM images.

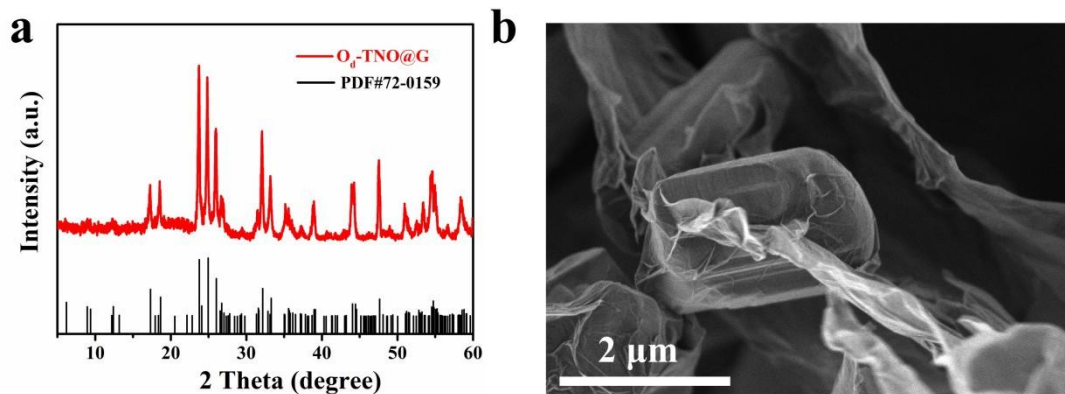


Fig. S3 Microstructure and morphology of O_d -TNO@G. (a) XRD pattern; (b) SEM images.

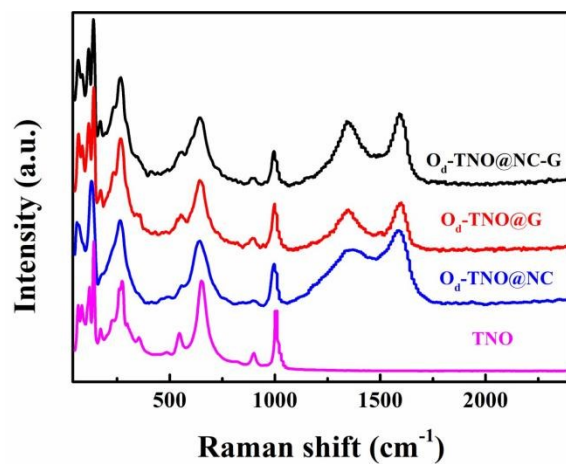


Fig. S4 Raman spectra of the TNO, O_d-TNO@NC, O_d-TNO@G and O_d-TNO@NC-G.

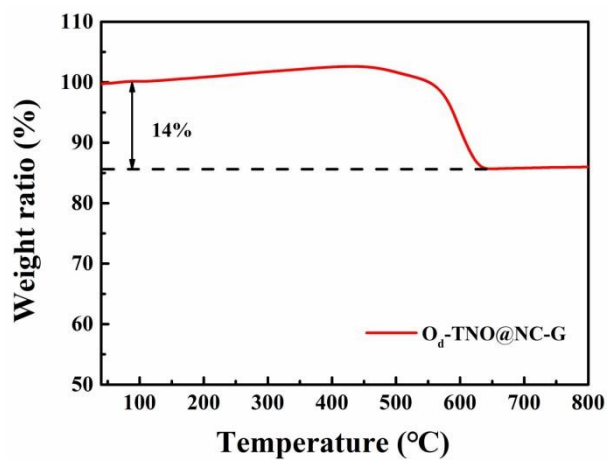


Fig. S5 TGA curve of O_d-TNO@NC-G.

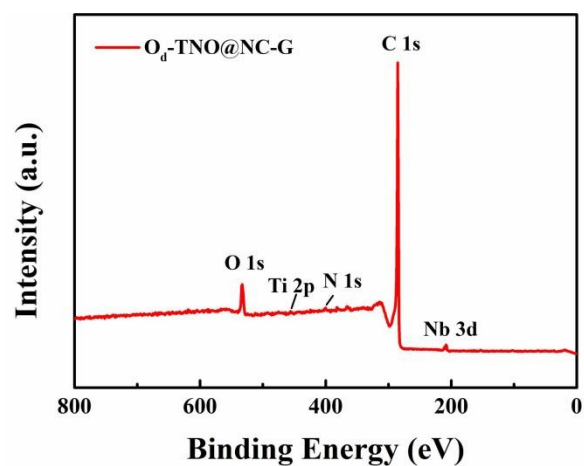


Fig. S6 XPS survey spectrum of O_d -TNO@NC-G.

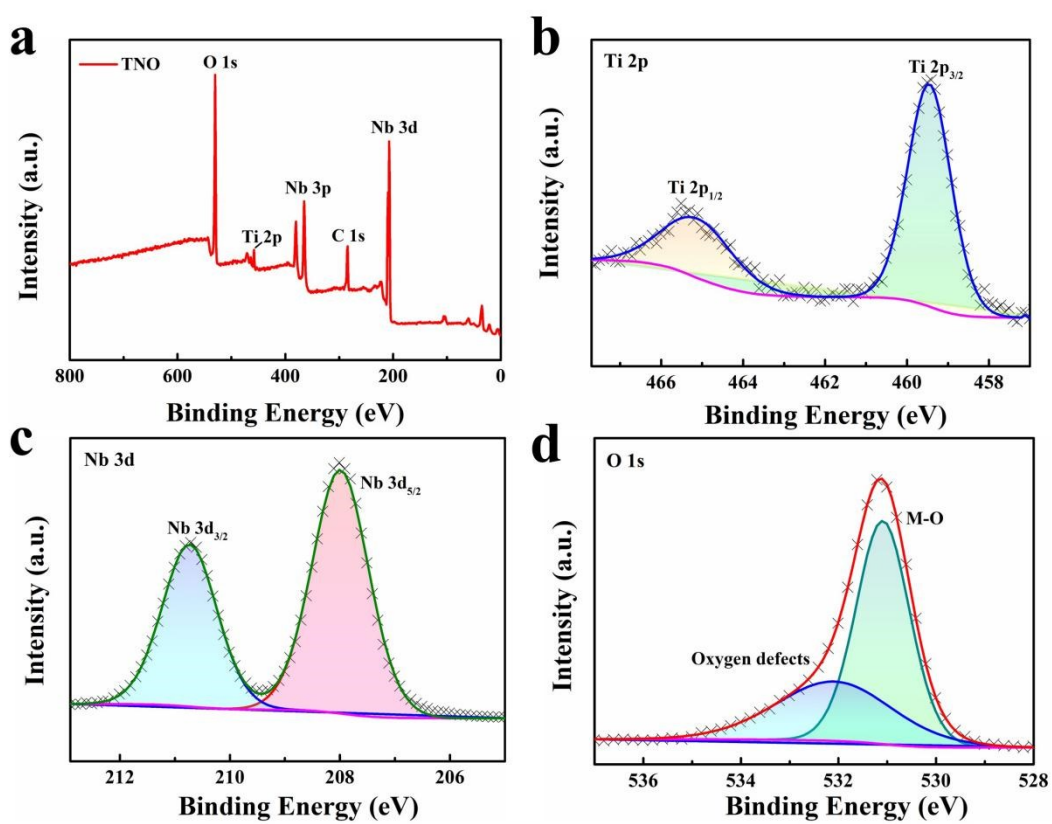


Fig. S7 (a) XPS survey spectrum of TNO; (b) Ti 2p; (c) Nb 3d; (d) O 1s.

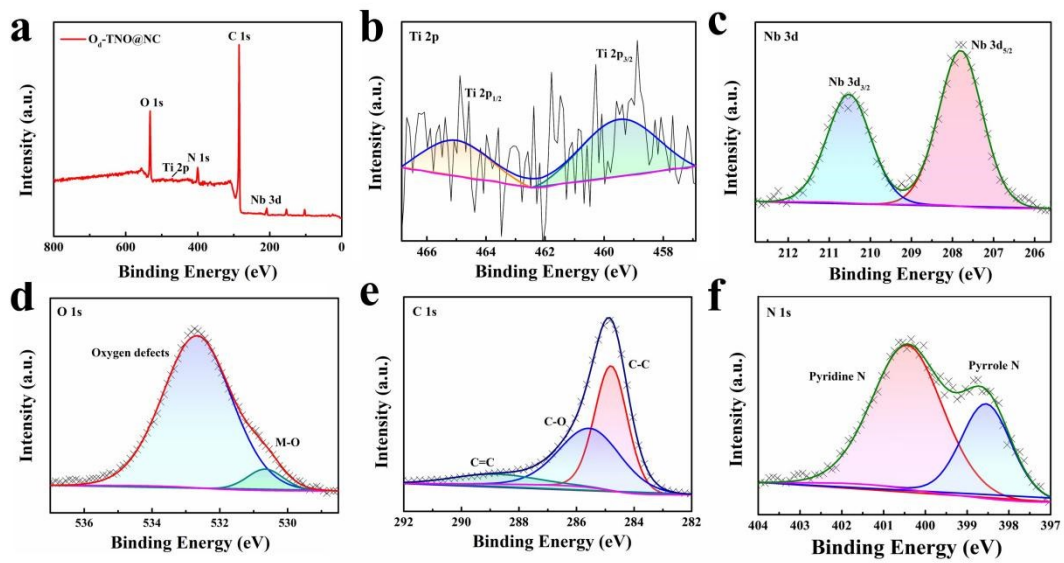


Fig. S8 (a) XPS survey spectrum of O_d -TNO@NC; (b) Ti 2p; (c) Nb 3d; (d) O 1s; (e) C 1s; (f) N 1s.

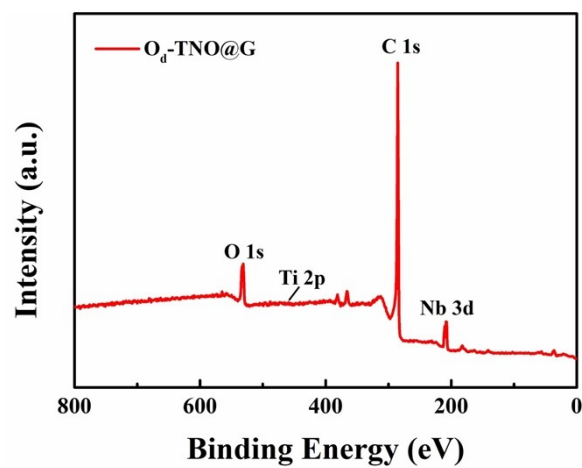


Fig. S9 XPS survey spectrum of O_d -TNO@G;

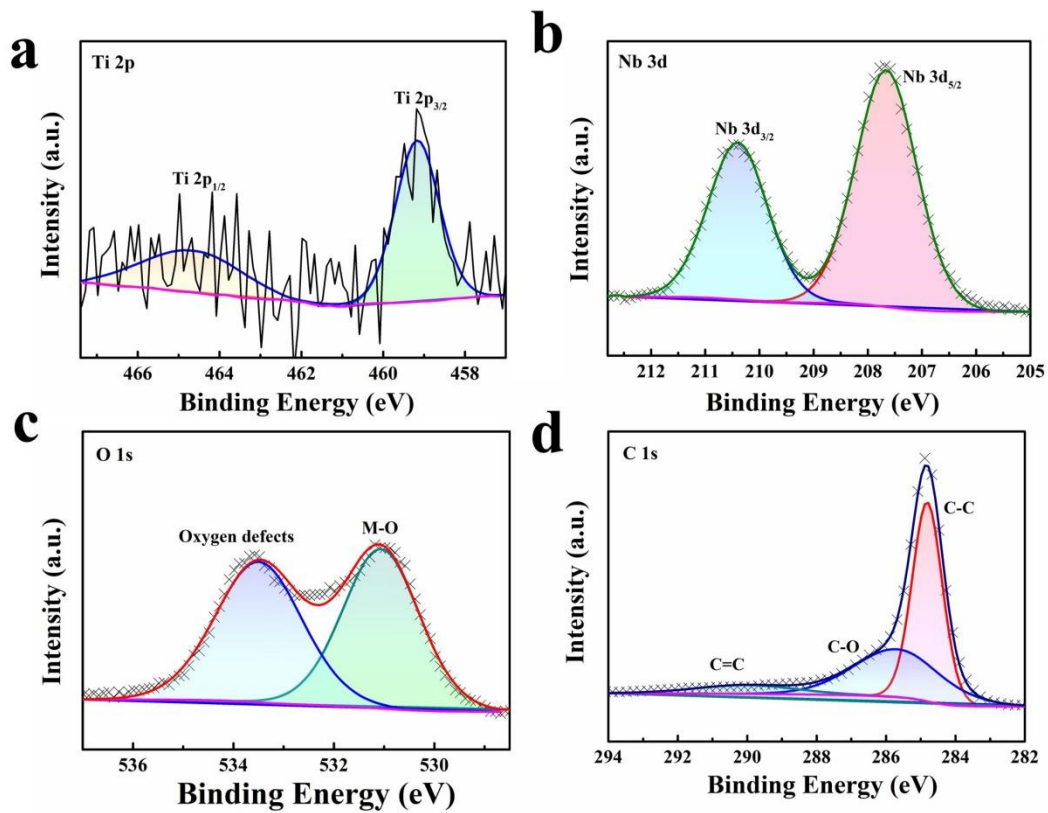


Fig. S10 XPS spectra of O_d -TNO@G; (a) Ti 2p; (b) Nb 3d; (c) O 1s; (d) C 1s.

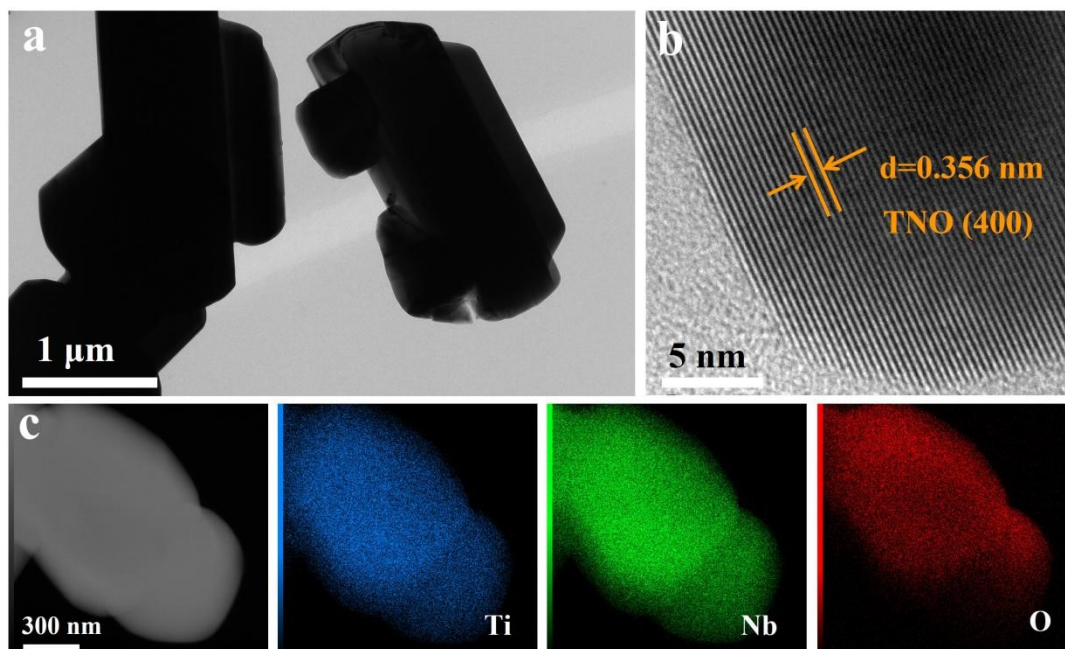


Fig. S11 (a) TEM and (b) HR-TEM images of the TNO; (c) HAADF-STEM image and EDX mappings of the TNO.

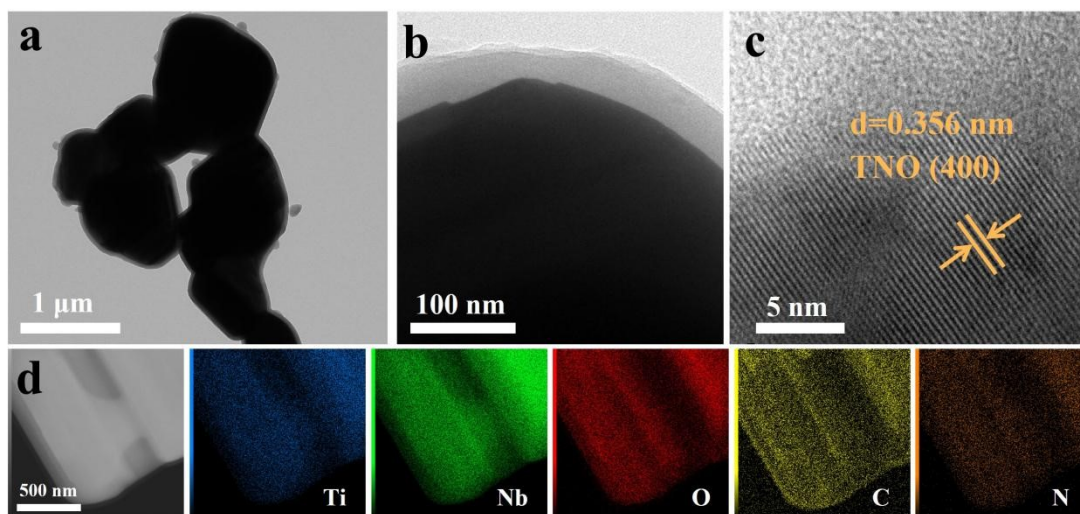


Fig. S12 (a and b) TEM and (c) HR-TEM images of the O_d -TNO@NC; (d) HAADF-STEM image and EDX mappings of the O_d -TNO@NC.

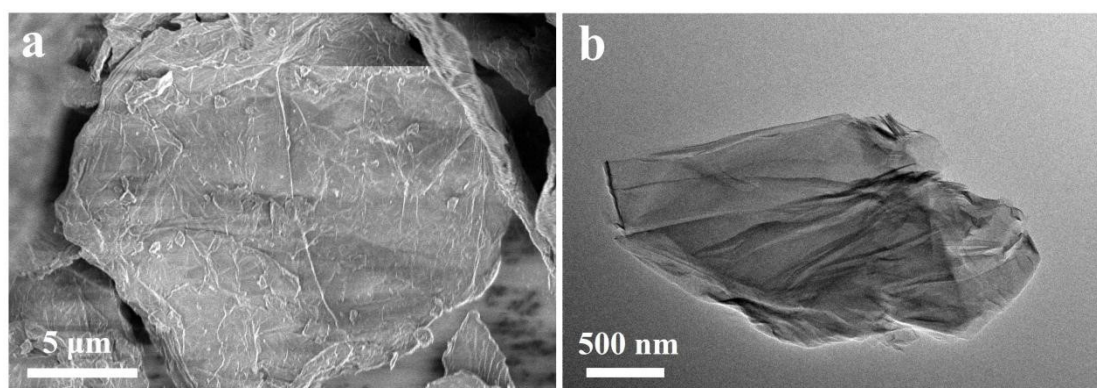


Fig. S13 (a) SEM and (b) TEM images of the GO.

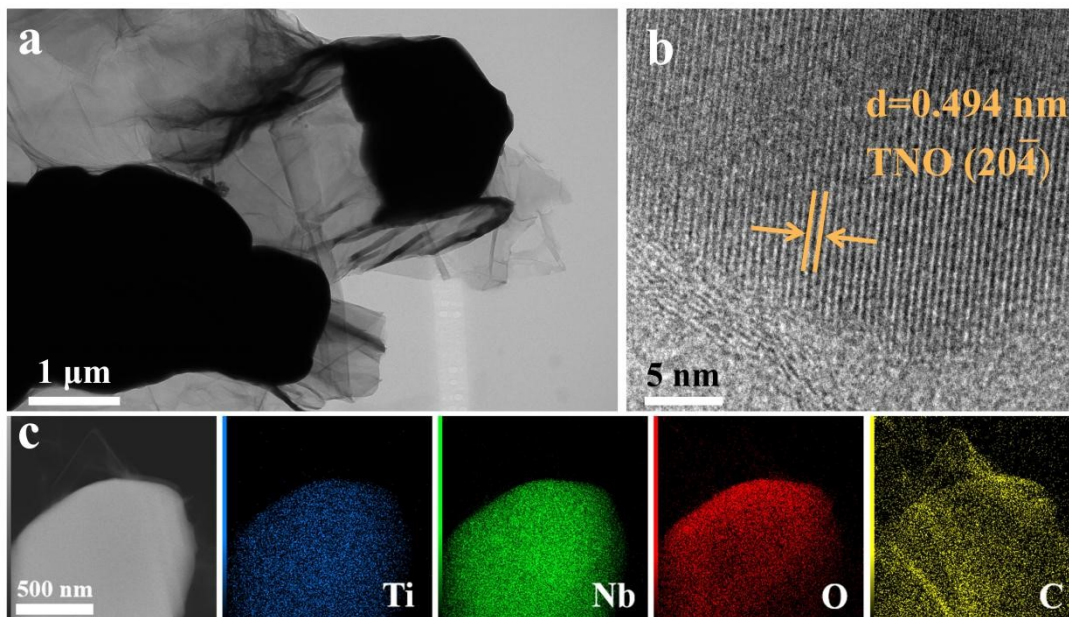


Fig. S14 (a) TEM and (b) HR-TEM images of the O_d -TNO@G; (c) HAADF-STEM image and EDX mappings of the O_d -TNO@G.

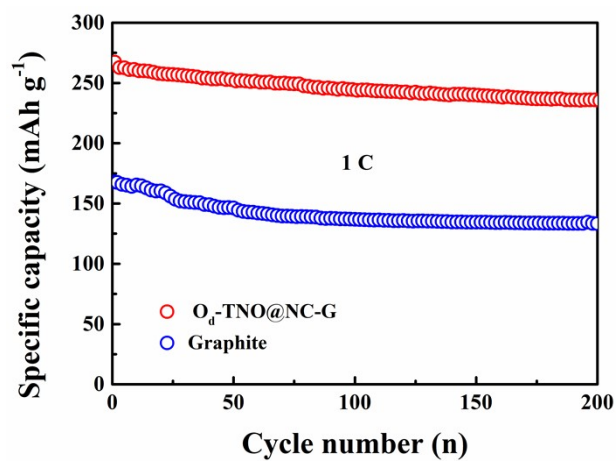


Fig. S15 Cycling performance at 1 C of the O_d -TNO@NC-G and commercial graphite (Hefei Kejing Material Technology Co., LTD, 99%).

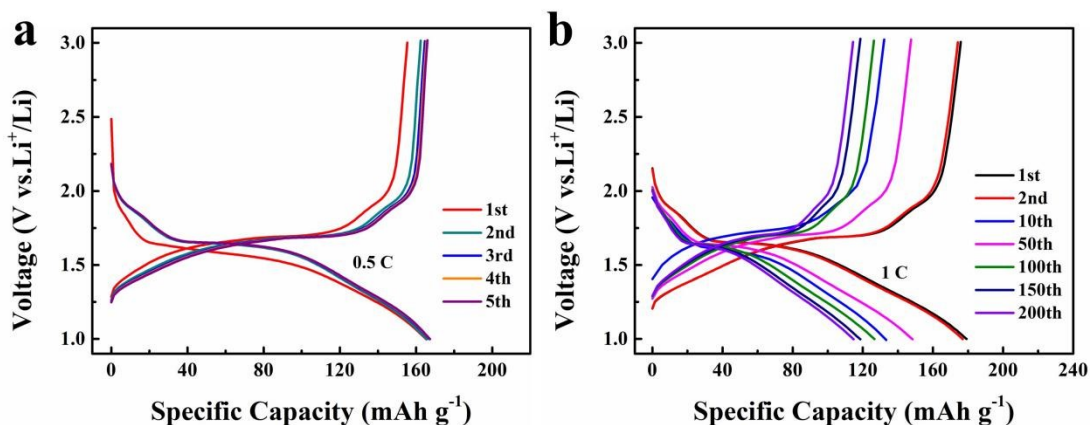


Fig. S16 (a) The GCD curves at 0.5 C and (b) typical charge–discharge curves at 1 C at different cycles of the TNO.

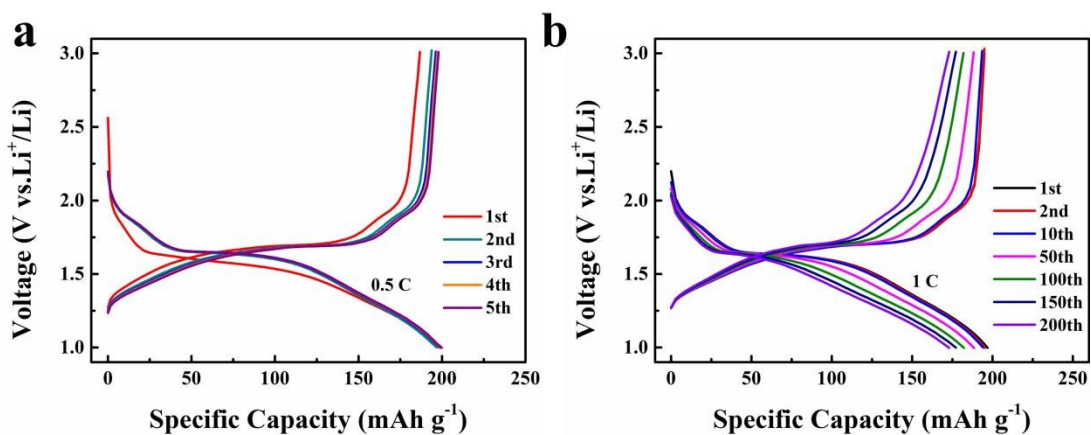


Fig. S17 (a) The GCD curves at 0.5 C and (b) typical charge–discharge curves at 1 C at different cycles of the O_d-TNO@NC.

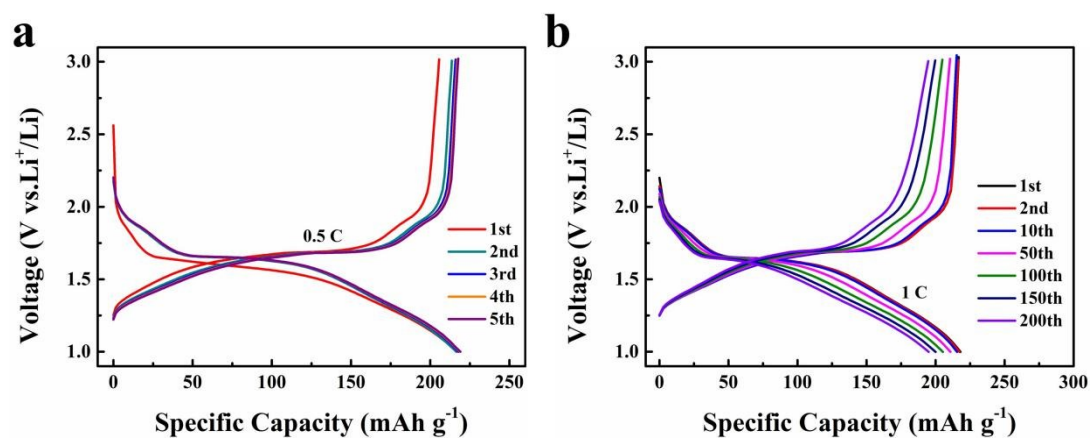


Fig. S18 (a) The GCD curves at 0.5 C and (b) typical charge–discharge curves at 1 C at different cycles of the O_d-TNO@G.

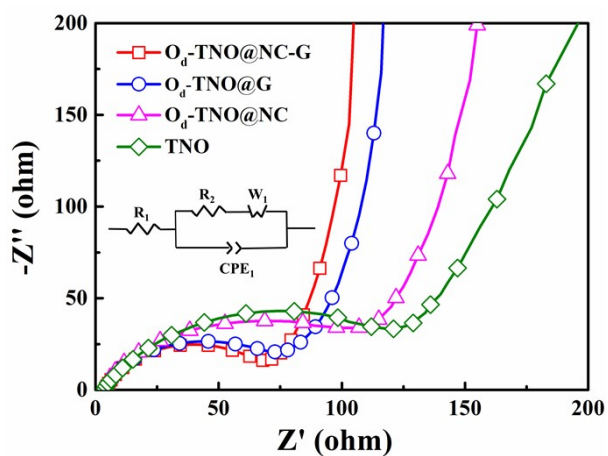


Fig. S19 EIS spectra of TNO, O_d -TNO@NC, O_d -TNO@G and O_d -TNO@NC-G (Inset is the corresponding equivalent circuit).

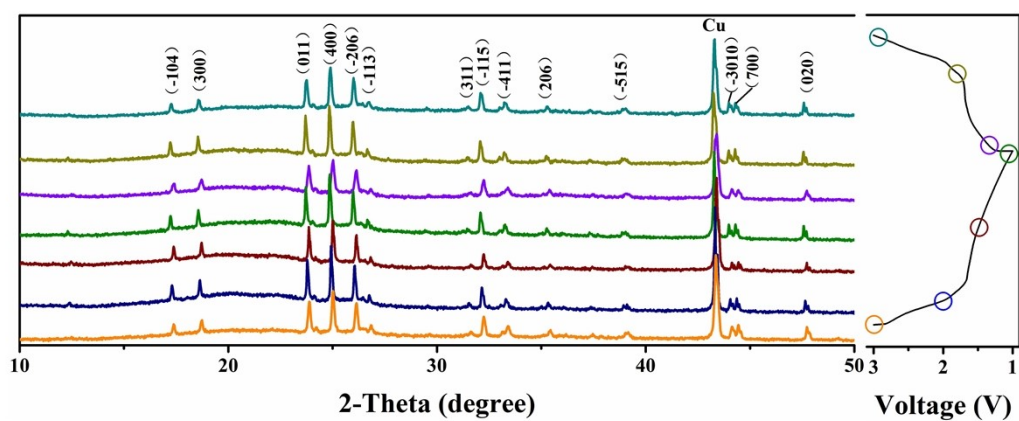


Fig. S20 Ex-situ XRD patterns of the O_d -TNO@NC-G anode measured at various discharge/charge states.